

Physics Analysis of the FIRE experiment

S.C. Jardin¹, C.E. Kessel¹, D. Meade¹, J. Breslau¹, G. Fu¹, N. Gorelenkov¹, J. Manickam¹, W. Park¹, H. Strauss²

¹Princeton Plasma Physics Laboratory, Princeton NJ 08540 USA

²Courant Institute of Mathematical Science, New York University, New York, NY

Introduction:

The proposed Fusion Ignition Research Experiment (FIRE) is a \$1B class facility that will be capable of exploring many of the burning plasma physics issues of interest to our community. The device dimensions can be “derived” from an optimization algorithm where we seek the most compact configuration that utilizes wedged copper alloy toroidal field coils pre-cooled to 80 °K and without active cooling [1]. The constraints imposed during the optimization include ELMy H-mode ITER98(y,2) scaling for the energy confinement time, a density limit of $n_{20} < 0.75 n_{GW}$, sufficient power to exceed the H-mode power threshold, a normalized stability parameter of $\beta_N < 1.8$, and a pulse length exceeding (by a factor of 2) that required for the plasma current profile to fully equilibrate to a stationary state. This leads to a reference design with $R_0 = 2.14$ m, $a = 0.595$ m, $B_t(R_0) = 10$ T, $I_p = 7.7$ MA with a flattop time at full parameters of 20 s, and with 150 MW of fusion power. The strong shaping ($\delta_X = 0.7$, $\kappa_X = 2.0$) and low normalized density can be expected to improve the confinement to a multiplier of 1.1 applied to the H98(y,2) global confinement time scaling, projecting to a fusion gain $Q \sim 10$ [2].

Core Transport and Boundary Conditions:

There are several transport models that have been developed for use in predicting the profiles and performance in a burning plasma. We have implemented three of the leading models in the TSC integrated modeling code [3] and used them to predict the performance of FIRE and the type of MHD behavior to expect. The three models are (A) the Multi-Mode Model MMM95 [4], (B) the Gyro-Landau Fluid model GLF23 [5], and (C) the “standard TSC” Coppi-Tang model [3]. These models are supplemented by a sawtooth model and boundary and edge models.

The H-mode models (A) and (B) are only applied in the central region $0 < \Phi < 0.75$, where Φ is the normalized toroidal magnetic flux that is zero at the magnetic axis and unity at the plasma/vacuum separatrix. In the edge region $0.75 < \Phi < 1.0$, we use an edge transport model $\chi_i = \chi_e = C/n_e$, where n_e is the local electron density and C is a constant chosen as $C = 2 \times 10^{19}$. The constant C has been chosen to make the pressure gradient in this region just below the infinite-n ballooning mode stability criteria. This leads to electron and ion temperatures at the top of the pedestal, $\Phi = 0.75$, of 4-5 KeV. For transport model (C), we impose a separatrix temperature at $\Phi = 1.00$ of $T_e = T_i = 400$ eV.

The density profile is not advanced in time in these simulations, but is rather a prescribed function of normalized poloidal flux, ψ , and time, t . We take the electron density to be $n_e(\psi, t) = n_0(t) \times [(1 - \psi^\beta)^\alpha + r_{edge}]$, with $\alpha = 0.3$, $\beta = 2.25$, $n_0 = 5.8 \times 10^{19}$ and $r_{edge} = 0.3$ during the current flattop. This leads to a line-averaged density of 0.60 times the Greenwald limit, and a ratio of peak to volume average of 1.15. We also include a uniform distribution of 3% Beryllium impurity, which together with the He buildup (assuming $\tau_p = 5$ sec), leads to a value of $Z_{EFF} \sim 1.4$ during the flattop.

Sawtooth Model:

One of the major uncertainties in the physics design of a burning plasma experiment is the behavior of the internal $m=1$ mode. We have implemented the Porcelli sawtooth model [6] in TSC and have investigated its consequences on transport and ignition. The nonlinear M3D code has been used to investigate the assumptions made in the Porcelli model and to evaluate the consequences of the sawtooth crash in FIRE-like devices, including the effects on the high-energy Helium population and the formation of stochastic regions outside the $q=1$ surface. In the present integrated modeling simulations, we assume that the surfaces outside the inversion surface remain good during the sawtooth activity.

The Porcelli sawtooth model triggers an event if one of the following 3 criteria is met:

$$-\delta\hat{W}_{core} > \omega_{Dh}\tau_A \quad (1)$$

$$-\delta\hat{W} > 0.5\omega_{*i}\tau_A \quad (2)$$

$$\hat{\rho} < -\delta\hat{W} < 0.5\omega_{*i}\tau_A \quad \text{and} \quad \omega_{*i} < \gamma_p \quad (3)$$

Here, $\delta\hat{W} = \delta\hat{W}_{core} + \delta\hat{W}_{fast}$, where $\delta\hat{W}_{core} = \delta\hat{W}_{mhd} + \delta\hat{W}_{KO}$. We have used the approximations in Ref. [6] for the various terms but have modified the coefficients by comparing them with the more exact results obtained by PEST and NOVA-K. We find that the Porcelli expression for $\delta\hat{W}_{fast}$ needs to be multiplied by $\sqrt{2}$ to get agreement with NOVA-K for this geometry.

The PEST calculations shows the importance of calculating the $\delta\hat{W}_{mhd}$ with the correct wall boundary condition, consistent with [8]. When the sawtooth is predicted to be triggered, we modify the transport coefficients in two ways. The value of the toroidal flux at the inversion

surface, Φ_1 , is calculated as
$$\int_0^{\Phi_1} \left(\frac{1}{q(\Phi)} - 1 \right) d\Phi = 0$$

For the duration of the sawtooth crash time τ_{CRASH} , we define the thermal conductivity and the hyper-resistivity to be: $\chi = \Gamma_1^2 / \tau_{CRASH}$ and $\lambda = \lambda_0 B_0^2 r_1^4 / \tau_{CRASH}$. A value of $\lambda_0 = 0.1$ effectively causes a Kadomtsev reconnection to occur [7] in the time $t = \tau_{CRASH}$, which we took to be 10 ms in these runs. By lowering λ_0 to 0.001, we can model an incomplete reconnection where the temperature profile flattens but the current and flux do not fully reconnect.

Discharge Simulation:

We have developed a full 1 1/2D TSC integrated simulation of a complete FIRE discharge including current rampup, flattop, burn, and current rampdown for each of the three transport models, and utilizing the Porcelli sawtooth model. We utilize a feedback system on the ICRH power designed to keep the total stored energy W constant at 34.5 MJ of total stored energy. Each of these simulations results in an energy multiplication factor $Q > 10$. Selected results are presented in Figures 1 and 2. Each of these 3 models leads to a different behavior of the sawtooth as shown in these figures. The model A (MMM95) has sawteeth every ~ 5 seconds triggered by the criteria in Eq. (3), the model B (GLF23) has sawteeth every ~ 7 seconds, triggered by the criteria in Eq. (2). In model C (Coppi-Tang), the sawteeth occur much more frequently, about every 0.5-second, and are triggered by the criteria in Eq. (1).

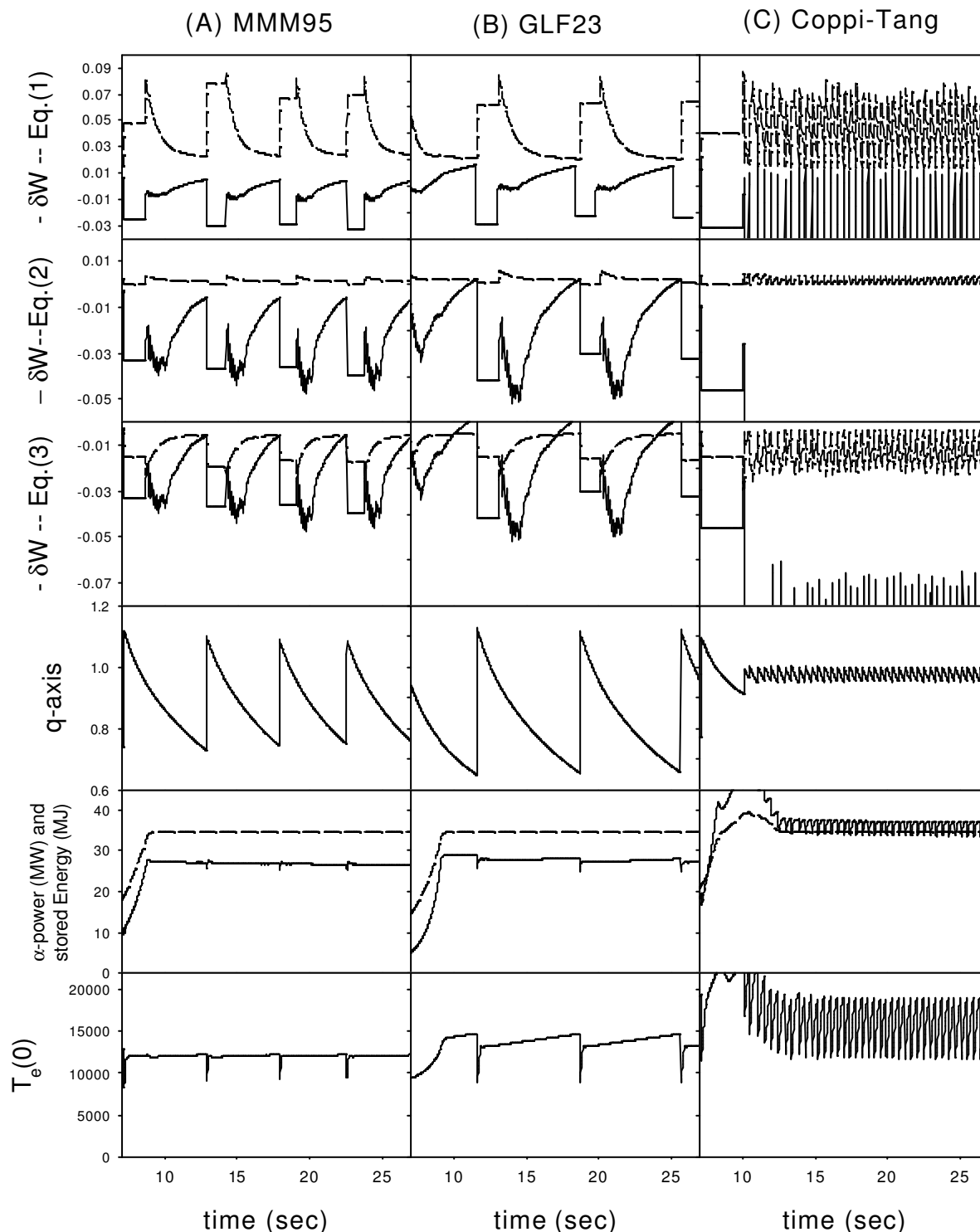
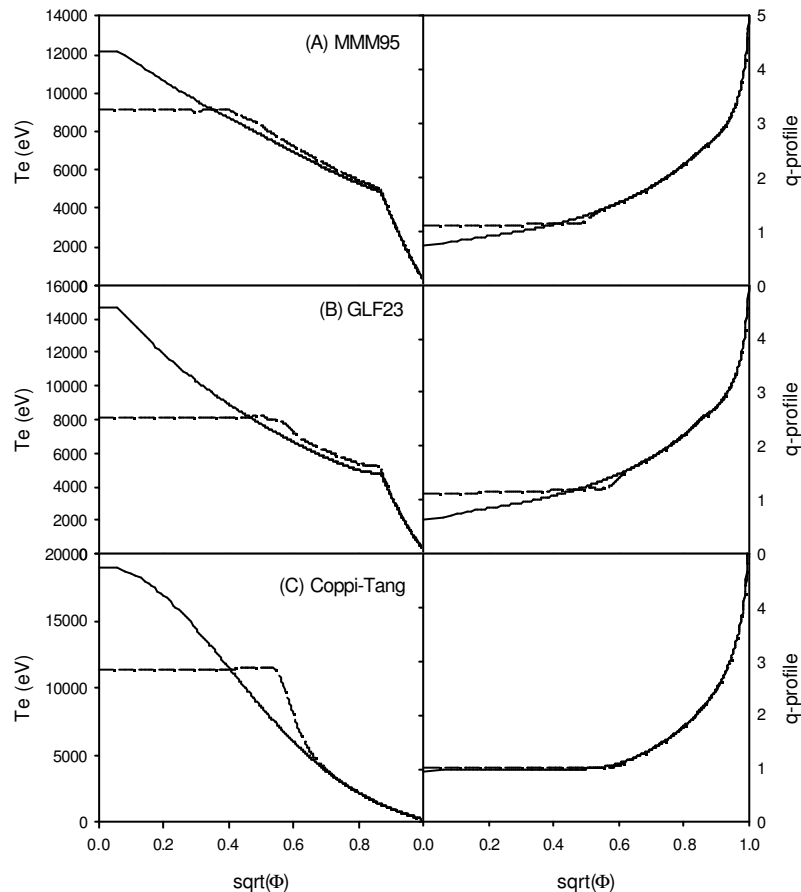


Figure 1: The top three frames show the appropriate $-\delta W$ from the Porcelli model (solid) and the critical value (dashed) for the 3 transport models for the 3 criteria corresponding to Eqns. (1)-(3). During the flattop, for the simulation using model (A), the sawtooth is triggered by criteria 3, for model (B) it is criteria 2, and for model (C) it is criteria 1. The 4th row shows the safety factor on axis for each of the 3 models. The final rows show the total stored energy (W) and the instantaneous α -power, and central electron temperature $T_e(0)$.

The electron temperature and safety factor profiles just before and after the last crash for these runs are shown in Figure 2. The instantaneous alpha power production and total stored energy are staying relatively constant in each of these runs, as shown in the bottom row of

Figure 1. When these runs are repeated but using the incomplete reconnection model ($\lambda_0 = 0.001$), we find very similar results, with the primary difference being the sawtooth frequency increases (2 sec, 3.5 sec, 0.2 sec) and the excursion in q_0 is less [(0.75, 90), (0.67, 90), (0.86, 89)], but the performance and Q value are essentially unchanged.

Figure 2: Electron temperature and safety-factor profiles just before (solid) and after (dotted) a sawtooth crash for the (A) MMM95, (B) GLF23, and (C) Coppi-Tang transport simulations with a complete reconnection.



Advanced Mode Operation:

Besides the reference inductive high-performance operating mode, the FIRE device is capable of operating at reduced parameters for longer times. The addition of a 20 MW LHCD system at 5.6 GHz will enable long pulse operation at reduced fields. Advanced tokamak configurations without relying on wall stabilization have been

modeled with $\beta_N=2.5$. We have used TSC/LSC to simulate a fully non-inductive discharge at a bootstrap fraction of up to 70% with a wall-stabilized $\beta_N = 3.5$ at fusion gain $Q > 5$. A close fitting copper-clad passive stabilizer provides $n=0$ and $n=1$ mode control.

Acknowledgements: The authors have benefited from discussions with G. Bateman, J. Kinsey, and A. Kritz. The MMM95 and GLF23 subroutines were downloaded from the NTCC modules library [<http://w3.pppl.gov/NTCC>]. This work was supported by DOE Contract # DE- AC02-76CHO3073.

REFERENCES

- [1] Jardin SC; Kessel C; Meade D; Neumeyer C; PPPL-3666 (to appear in Fus Eng and Des)
- [2] J.G. Cordey, et al., Proc. 28th EPS Conf. On Con. Fus. And Plas Phys., 2001, paper 3.11
- [3] Jardin SC; Bell MG; Pomphrey N; Nucl Fusion 33 (1993) 371
- [4] Bateman, G; Kritz AH; Kinsey JE; ReDD AJ, Physics of Plasmas **5** (1998) 2355
- [5] Waltz R; et al, Phys. Plasmas **4** (1997) 1499
- [6] Porcelli F; Boucher D; Rosenbluth M; Plas. Phys. and Cont. Fusion **38** (1996) 2163
- [7] Ward DJ and Jardin SC Nucl Fusion **29** (1989) 905
- [8] Lutjens H; Bondeson A; Vlad G; Nucl Fusion 32 (1992) 1625